Sensor-scheduling simulation of disparate sensors for Space Situational Awareness

Tyler A. Hobson
School of Information Technology & Electrical Engineering
The University of Queensland
I. Vaughan L. Clarkson
School of Information Technology & Electrical Engineering
The University of Queensland

ABSTRACT

The art and science of space situational awareness (SSA) has been practised and developed from the time of Sputnik. However, recent developments, such as the accelerating pace of satellite launch, the proliferation of launch capable agencies, both commercial and sovereign, and recent well-publicised collisions involving man-made space objects, has further magnified the importance of timely and accurate SSA.

The United States Strategic Command (USSTRATCOM) operates the Space Surveillance Network (SSN), a global network of sensors tasked with maintaining SSA. The rapidly increasing number of resident space objects will require commensurate improvements in the SSN. Sensors are scarce resources that must be scheduled judiciously to obtain measurements of maximum utility. Improvements in sensor scheduling and fusion, can serve to reduce the number of additional sensors that may be required.

Recently, Hill et al. [1] have proposed and developed a simulation environment named TASMAN (Tasking Autonomous Sensors in a Multiple Application Network) to enable testing of alternative scheduling strategies within a simulated multi-sensor, multi-target environment. TASMAN simulates a high-fidelity, hardware-in-the-loop system by running multiple machines with different roles in parallel. At present, TASMAN is limited to simulations involving electro-optic sensors. Its high fidelity is at once a feature and a limitation, since supercomputing is required to run simulations of appreciable scale.

In this paper, we describe an alternative, modular and scalable SSA simulation system that can extend the work of Hill et al with reduced complexity, albeit also with reduced fidelity. The tool has been developed in MATLAB and therefore can be run on a very wide range of computing platforms. It can also make use of MATLAB's parallel processing capabilities to obtain considerable speed-up. The speed and flexibility so obtained can be used to quickly test scheduling algorithms even with a relatively large number of space objects.

We further describe an application of the tool by exploring how the relative mixture of electro-optical and radar sensors can impact the scheduling, fusion and achievable accuracy of an SSA system. By varying the mixture of sensor types, we are able to characterise the main advantages and disadvantages of each configuration.

1. INTRODUCTION

For over half a century, the Earth-Orbiting-Satellite population has consistently risen. Along with each satellite has come a trail of rocket stages, separation devices, fairings and rocket exhaust products that are typically discarded and left to drift about the Earth. The resulting cloud of man-made objects orbiting around the Earth at great speed and along a variety of trajectories threatens to collide with space-borne assets the world has become reliant upon for enabling microgravity research, telecommunications, weather forecasting, Earth observations and navigation. Crucially, the problem is expected to increase in severity for the foreseeable future. The ability to effectively detect and track these objects for mission planning and collision avoidance is therefore of increasing significance.

Groups such as United States Strategic Command (USSTRATCOM) have endeavoured to maintain Space Situational Awareness (SSA) by tracking all man-made objects since the 1950s. The continual growth of the Resident Space Object (RSO) population necessitates USSTRATCOM's strategy for staying one step ahead. By commissioning research regarding the improvement of SSA maintenance capabilities before it is necessary, USSTRATCOM aim to meet future demand. Due to the enormous overheads associated with trialling improved methodologies for maintaining SSA using an existing sensor network for space surveillance (SNSS), it is a logical choice to initially simulate the problem, to permit efficient research of an optimal solution. Initial attempts at this

simulation, are described in a recent paper by Hill et al. [1] who have named their simulation Tasking Autonomous Sensors in a Multiple Application Network (TASMAN).

To ensure comparable results to experimentation with a genuine SNSS are produced, TASMAN has been designed to imitate reality as closely as possible. TASMAN simulates a high-fidelity, hardware-in-the-loop system that maintains an RSO catalogue of manmade objects orbiting the Earth. This system is realised by running multiple machines with different roles in parallel. These roles include orbit determination, truth orbit propagation, object catalogue preservation as well as sensor modelling and mission planning. TASMAN achieves its high fidelity information from well-established orbit propagators and physics engines. Creating this level of fidelity however, necessitates supercomputing, which inflates the cost and timeline required for researching and testing alternative methods.

This paper describes a new tool for SSA research named MASSAS or MATLAB Space Situational Awareness Simulation. MASSAS's purpose is the timely and efficient characterisation of alternative SSA maintenance methodologies with a reduced focus on high fidelity simulation. For this reason MASSAS was designed to produce similar results to TASMAN [1] while only requiring low fidelity models and a single computer running MATLAB. MASSAS has also been designed for modularity, to enable efficient addition or modification of its constituent components. As a demonstration of this ability, this paper also presents a characterisation study of optical and radar SSA sensors by means of interchanging the system sensor model. It is proposed that with this tool, competing methods and alternative approaches can be researched and characterised with significantly less resources and in a reduced amount of time. In addition, when an optimal approach is achieved, fidelity can be increased for performance prediction prior to incorporation into high fidelity simulations such as TASMAN or a true SNSS.

The paper begins with a general description of the methods used to develop and evaluate TASMAN by Hill et al. that are necessary for reproduction on MASSAS for comparison of results. The subsequent section provides an overview of the development of MASSAS paying special interest to any differences between the simulations. The result of consequent comparative tests between TASMAN and MASSAS are revealed in the following section. In addition, results of comparative tests between MASSAS's optical and radar models used in a number of configurations are also produced. Conclusions are drawn in the final section as to the viability of the proposed low-fidelity research and ideas for proposed future work are discussed.

2. TASMAN RESULT REPLICATION

To ensure MASSAS can deliver comparable results to TASMAN, MASSAS was initially configured to simulate the same methodologies and initialisation parameters as chosen by Hill et al. [1].

2.1 Simulation Initialisation

TASMAN's recent results [1] were produced by performing a number of 8-day simulations. A tasking period of 24 hours was used for mission planning of sensors. After each tasking period, the catalogue was reassessed and mission planning for the next period commenced. Observations of RSOs were obtained exclusively by simulated electro-optical sensors which provided 120 second tracks, consisting of five angle pairs representing right ascension and declination.

TASMAN truth orbits and state information for the RSO catalogue [1] were obtained from the Space-Track website [2] in the form of Two Line Element (TLE) sets on December 15, 2009. The list of RSOs to be catalogued for the simulation was selected using the criteria found in Table 1.

Table 1. Criteria for selection of simulated RSOs

	Semi-major axis (km)	Eccentricity	Inclination (deg)	Radius of perigee (km)
Minimum	25 000	0	50	25 000
Maximum	28 000	0.05	70	28 000

The resulting list of Medium Earth Orbit (MEO) objects contained 214 entries. The 214 object TLEs were again obtained from the Space-Track website [2] for the purposes of ensuring the results of this paper are comparable.

The state vector chosen for this paper is,

$$\mathbf{x} = \begin{bmatrix} x & y & z & \dot{x} & \dot{y} & \dot{z} \end{bmatrix}^T \tag{1}$$

consisting of three position and three velocity components in rectangular Earth centred, inertial coordinates and is consistent with Hill et al.'s approach [1]. RSO catalogue state estimate $\hat{x}$ and covariance P were artificially devised by means of Gaussian random value generators with standard deviations of σ_P and σ_v. The generated random values were appropriately assigned to a 6×1 vector Δx enabling computation of the resulting state estimate using

$$\hat{x} = x + \Delta x. \tag{2}$$

σ_P and σ_v were chosen sufficiently large to test the method's ability to improve the RSO catalogue from a poor state of maintenance. Initial independence assumptions enabled the generation of the 6×6 covariance matrix P by,

$$P = diag\begin{bmatrix} \sigma_p^2 & \sigma_p^2 & \sigma_p^2 & \sigma_v^2 & \sigma_v^2 & \sigma_v^2 \end{bmatrix}. \tag{3}$$

Sensor functionality was intentionally limited to ensure simulated observations were physically realisable by existing hardware. The limitations imposed on sensors by terrestrial occlusion and atmospheric distortion were realised by restricting sensors from obtaining observations at elevations lower than 20 degrees above horizontal. Optical sensor angle pairs obtained from truth data were each added with one arc second standard deviation of random Gaussian error. In addition, each sensor was limited to a maximum of 200 observations per tasking period. This limitation was applied to ensure the resulting relative accuracies were solely a consequence of effective sensor scheduling.

Sensor locations were selected at authentic space surveillance sites that also provide adequate global coverage. In agreement with Hill et al. [1], the selected sites are presented in Table 2.

Table 2. Sensor Site Locations

Site	East Longitude (deg)	North Latitude (deg)	Height Above Ellipsoid* (m)
Kwajalein, Pacific Ocean	167.7333[†]	8.716667	50
Albuquerque, USA	253.502717	34.96305	1725
Moron, Spain	354.41194	37.1511	101

2.2   SSA Methodologies

Hill et al. [1] presented three alternate sensor network tasking/scheduling methodologies named Scenario 1-3. The principal differences between each scenario were defined by the network topology and the availability of data throughout the simulated SNSS.

Scenario 1

The first scenario is designed to imitate the mission planning strategies implemented by USSTRATCOM's own SNSS named the Space Surveillance Network (SSN) [1]. Tasking is performed in the same geographical location as the RSO catalogue is compiled. Crucially, although the tasker has access to the RSO catalogue and the orbit error covariance information contained within, it has only rudimentary knowledge of each sensor's capabilities. The tasker creates a prioritised list of objects to be passed onto the scheduler by assigning each object to a category according to its orbit error covariance. Each scheduler is co-located with a sensor and has detailed knowledge of its sensor's capabilities. Each scheduler/sensor pair is placed at geographically disparate locations, providing adequate global coverage. Each scheduler progresses through the tasking list and determines when to observe an object. Scheduling is accomplished through the application of sensor specific weighting criteria designed to achieve optimality with the available data. Scheduling criteria include probability of detection, target visibility overlap and remaining opportunities for orbit observation diversity.

Scenario 2

Although the RSO catalogue remains centralized in Scenario 2, the distinction between tasker and scheduler is lost as the role of the tasker is effectively absorbed into each scheduler. In addition, each scheduler now has access to the orbit error covariance information contained in the RSO catalogue. This enables the schedulers to take advantage of a covariance based, observation effectiveness scheduling algorithm further explained in section 2.3. Covariance based scheduling enables the schedulers to not only select the RSO in most need of observation, but also decide

---

* Elliptical Earth model assumed World Geodetic System – 1984 (WGS-84).
† The East longitude for Kwajalein was erroneously published [1] as 192.2667 degrees.

when to make an observation to achieve the greatest reduction in orbit error covariance. Additionally, once each scheduler has chosen an object and an appropriate time, the scheduler can predict how the newly scheduled observation will affect the observation effectiveness of the same object at an alternate time. This feat is achieved by reverse time propagation of the predicted object covariance and enables the scheduler to effectively assign multiple observations to the same object within a single observation period. The weakness of this Scenario however is the lack of coordination between schedulers. Each scheduler does not know how the schedules of other sensors will affect the catalogue. This results in redundant observations of some objects from multiple sites, which has the secondary effect of reducing the total number of objects that could have been observed for maximum benefit.

Scenario 3

The final scenario introduces the centralized mission planner which performs the role of tasker and scheduler for all sensors. The mission planner has access to the RSO catalogue as well as detailed knowledge of each sensor's capabilities. Similar to Scenario 2, the mission planner uses a covariance based, observation effectiveness metric to perform tasking and scheduling. The vital difference however, is the mission planner's ability to overcome Scenario 2's weakness by comparing the observation effectiveness of all sensors for a single RSO. Scenario 3's mission planner can therefore predict how the scheduling of a sensor-object-time combination will affect the orbit error covariance of a catalogued RSO and use this prediction when performing subsequent scheduling.

2.3 Covariance Based Scheduling

The observation effectiveness method employed by TASMAN [1] for mission planning was devised from a fusion of methods presented by Blackman [3] and Tapley [4] resulting in multi-target covariance based sensor scheduling. The chosen technique employs the measurement update of an Extended Kalman Filter (EKF) [4] or Unscented Kalman Filter (UKF) [5-7] to determine a value representative of the reduction in 3D position error variance from a single observation. The applicable EKF measurement update equations are,

$$K_k = P_{k|k-1}H_k^T(H_kP_{k|k-1}H_k^T + R)^{-1} \tag{4}$$

$$\text{and } P_{k|k} = P_{k|k-1} - K_kH_kP_{k|k-1}. \tag{5}$$

Where K is the Kalman gain, H is the observation model and $[]^T$ denotes the matrix transpose operator. $P_{k|k-1}$ is the covariance matrix produced by the time update while $P_{k|k}$ is the measurement update covariance matrix. The matrix R is the measurement noise covariance matrix. The measurement errors are assumed independent and identically distributed (i.i.d.) Gaussian noise. The standard deviations of optical measurements right ascension and declination denoted as σ_α and σ_δ respectively. R is therefore generated by implementing

$$R = \begin{bmatrix} \sigma_\alpha^2 & 0 \\ 0 & \sigma_\delta^2 \end{bmatrix}. \tag{6}$$

Notably in Eq. (5), the updated covariance equals a priori covariance minus the matrix $K_kH_kP_{k|k-1}$. The matrix $K_kH_kP_{k|k-1}$ is therefore the predicted reduction in covariance due to a measurement update. The orbit update effectiveness metric, denoted β_{red}, is computed by obtaining a scalar representation of the position component of the matrix $K_kH_kP_{k|k-1}$. Noting the state element positions in Eq. (1), β_{red} is obtained by taking the 3×3 trace of the upper left quadrant of the 6×6 covariance reduction matrix $K_kH_kP_{k|k-1}$ as follows

$$\beta_{red} = tr\left(\left[K_kH_kP_{k|k-1}\right]_{p,3\times3}\right). \tag{7}$$

Alternatively if a UKF is used, β_{red} can be obtained by using P_{vv}, the innovations covariance matrix [1] by using

$$\beta_{red} = tr\left(\left[K_kP_{k|k-1}^{vv}K_k^T\right]_{p,3\times3}\right). \tag{8}$$

The UKF method presented in Eq. (8) was used for observation effectiveness computation for this paper. The covariance based scheduling method, enables the computation of the β_{red} observation effectiveness metric at all possible observation epochs during each tasking period. This method enables the scheduler to pick the most appropriate time to schedule an observation to have the greatest effect on the orbit error covariance. The result however is admittedly suboptimal, as it tends to favour observation late in the tasking period, once the error has had

time to grow [1]. This characteristic affords the scheduler a behaviour which focuses on error reduction rather than minimisation, which necessitates effective observation at the earliest opportunity.

2.4 Catalogue Accuracy

The final noteworthy parameters to be replicated by this paper for comparative purposes are the catalogue accuracy metrics, which are computed throughout the simulation to determine the state of the catalogue. Two metrics are defined by Hill et al. [1]; Catalogue Median and Catalogue Worst Case. Both metrics are obtained by firstly determining the largest 3D position error between the propagated truth and catalogue estimated states of each RSO over the prevailing 24 hour period. Once these errors are compiled, Catalogue Median and Catalogue Worst Case are then obtained by computing the median and maximum of the compilation.

3. MATLAB SSA RESEARCH TOOL

3.1 Research Environment

MASSAS is a MATLAB program, written to simulate an SNSS attempting to maintain SSA. It is flexible in functionality, due to high levels of modularity, as well as computation, due to advanced control over data storage and parallel processing afforded by the use of a high level language. Because of MASSAS's adaptability, components such as tasking/scheduling modules, sensor models, orbit propagators, orbit determination modules, physics modules and visualization features can be easily and/or dynamically interchanged and adapted to varying grades of fidelity. The flexibility afforded enables a large degree of control over simulation efficiency.

3.2 Truth Data

Depending on computational power and scenario constraints, MASSAS can be modified so that truth data is precompiled or dynamically evaluated during simulation. The benefit of precompiled truth data is the reduction of execution time when running alternate scenarios with the same initialisation parameters. Due to the specified scenario constraints, MASSAS has been configured to precompile with 30 second temporal resolution.

Similar to TASMAN [1], simulated truth orbit data is obtained from TLEs by performing simplified mean orbital element conversions to Cartesian positions and velocities. Subsequent conversion from the six Keplerian orbital elements to Cartesian elements provides the initial truth state vector of the object. Once established, propagation of state vectors and the application of sensor models enable computation of observation angles and object visibility at desirable epochs.

3.3 Orbit Propagation

High fidelity orbit propagation is a very complex and costly exercise [8]. This is exaggerated by the amount of orbit propagation necessary for computation of truth orbits, observation effectiveness, orbit determination and catalogue accuracy metrics in TASMAN and MASSAS. Because of the approximations made in the scenario methodologies, the current length of simulation and the important fact that both truth orbit data and orbit determination models are configured to use the same propagator, there is arguably little to be gained from high fidelity propagation when the cost is so high.

For the reasons considered, MASSAS was configured to use the very simple two-body Keplerian orbit propagation model presented by Vallado [8]. As necessary, the propagator's complexity can be increased to account for assumption changes such as the inclusion of high-drag low-earth-orbit (LEO) objects or increased simulation duration.

3.4 Sensor Model

MASSAS and TASMAN use sensor models to identify if and to what quality a particular sensor will be capable of obtaining an observation of an RSO. An important difference between MASSAS and TASMAN is the emphasis on alternative sensor model integration. Therefore as an initial step, MASSAS has been supplemented with a simplified radar sensor model in addition to an optical sensor model.

Furthermore, it is postulated [8, 9] that due to differences in observational information and accuracy, optical and radar observations provide disparate yet complimentary orbit track update information. In the absence of observation diversity, optical sensors are likely to reduce in-track error while supplying poor radial information due to accurate angle measurement and the absence of range data. Conversely radar is likely to provide increased radial error performance while lacking precision for in-track error reduction due to accurate range determination, yet inferior angle information.

Optical

The optical sensor model provides highly accurate angle measurements using passive optically visible radiation. The optical sensor model therefore relies on knowledge of sensor capability as well as a solar illumination model. The solar illumination model requires spatial knowledge of the Sun, Earth, sensor site and RSO. With this information, factors influencing illumination of the RSO such as solar eclipse, sensor/RSO phase angle[‡] and sensor-nightfall are computed. The complexities of a high fidelity illumination model are simplified with a number of rudimentary conditions such as a single solar light source, optimal weather, negligible light time, uniform RSO illumination and a conical Earth shadow model for eclipse and nightfall.

Radar

In contrast to the optical model, the radar model employed for this paper requires only knowledge of each sensor's specific capabilities. Radars in general can return a number of alternative observation parameters [8]. However the initial model will provide three parameters: range, azimuth and elevation measurements. Each radar measurement for this paper has i.i.d. Gaussian noise added to produce an error standard deviation of 30 metres for range and 54 arc seconds for angle as representative error values from genuine SSN radars [3, 9].

3.5 Orbit Determination

The problem of orbit determination is very old, yet the breadth of methods continues to expand today [3, 8]. Because each method has its own unique benefits and disadvantageous and because the initial aim of this study is to compare results with TASMAN [1], the chosen method of orbit determination implemented for this paper is achieved through the use of a UKF. The UKF is relatively simple to implement requiring knowledge only of the nonlinear equations,

$$x_k = f[x_{k-1}, v_{k-1}, k] \tag{9}$$

$$y_k = h[x_k, k] + w_k \tag{10}$$

where $k-1$ represents the previous state update epoch, k the observation epoch, x represents the $n \times 1$ state of the system, f is the state propagation model, v the process noise, y is the $m \times 1$ measurement vector, h relates the system state to the observation model and w the measurement noise. It is assumed that the noise vectors v_k and w_k contain zero-mean i.i.d Gaussian noise, and

$$E[v(i)v^T(j)] = \delta_{ij}Q(i), \quad E[w(i)w^T(j)] = \delta_{ij}R(i),$$
$$E[v(i)w^T(j)] = 0, \quad \forall i, j. \tag{11}$$

The particular implementation of the UKF used for this paper has been customised for this study to ensure robust operation when subjected to the chosen artificially induced noise. Due to Gaussian noise and six state parameters, $n = 6$, the scalar weighting parameter λ [6] has been assigned the value -3, in accordance with the equation,

$$\lambda = 3 - n. \tag{12}$$

Ideally, employing this method minimizes the mean-squared-error up to the fourth order. It is however acknowledged that after nonlinear transformation, the probability distribution is no longer Gaussian and sub-optimal solutions may result. It was empirically determined however that λ = -3 provided a consistently stable result. Stability was also enhanced by introducing a modified form of covariance evaluation [5] that prevents the matrix P_{yy} from losing positive definiteness due to a negative value for λ. Modification is achieved by changing covariance evaluation about the estimated mean to evaluation about a central sigma point. The central sigma point is positioned, prior to transformation, at the a priori system state mean.

Intuitively, if an alternative sensor is used, observation function h(.) and R must be appropriately adapted to represent the appropriate observation model. In the case of radar, a range parameter is computed in h(.) and appropriate measurement covariance information is added as a first row and column of R.

[‡] For the purposes of this paper, phase angle is defined as the angle between the site-sun and site-RSO vectors.

4. RESULTS

The catalogue initialisation noise statistics suggested by Hill et al. [1] was σ_P equal to 1×10^3 m and σ_v equal to 1×10^{-4} ms^{-1}. It was empirically determined however that values σ_P equal to 3.5×10^3 m and σ_v equal to 1×10^{-4} ms^{-1} were necessary to achieve a proportionate Catalogue Median. The results presented show the catalogue metrics, Catalogue Worst Case and Catalogue Median for both systems at the end of each 24 hr tasking period.
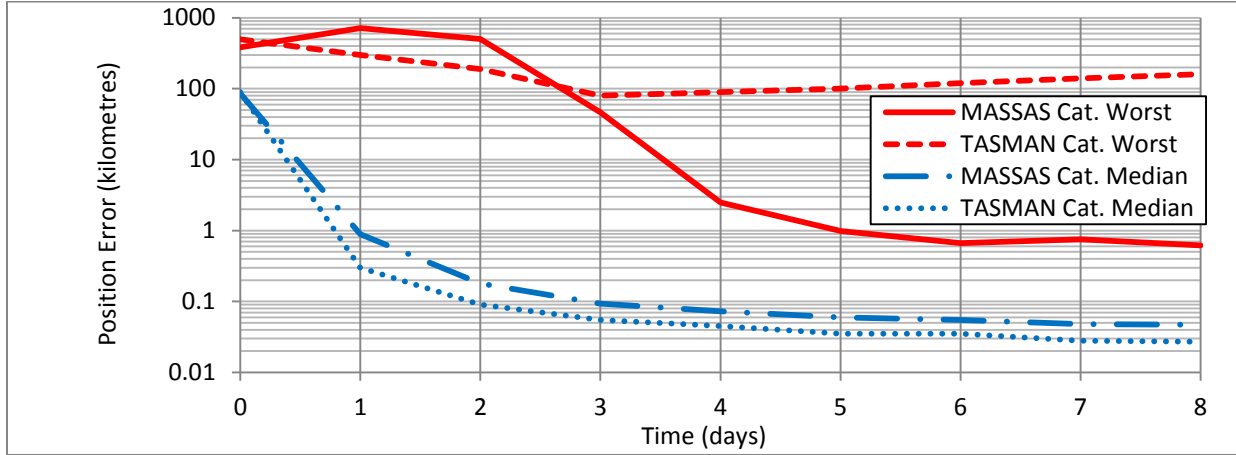
Fig. 1. MASSAS-TASMAN Comparison - Scenario 1
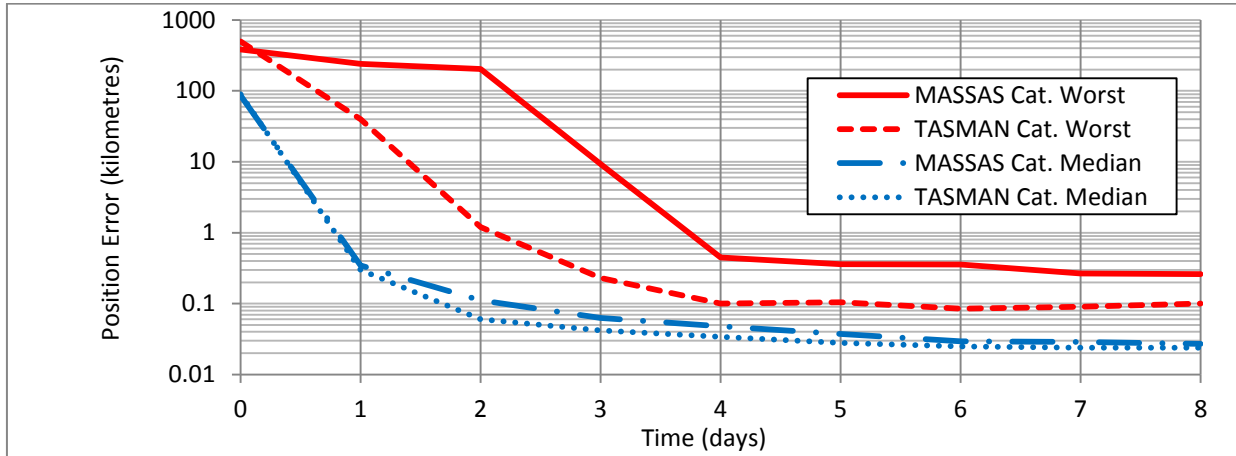
Fig. 2. MASSAS-TASMAN Comparison - Scenario 2
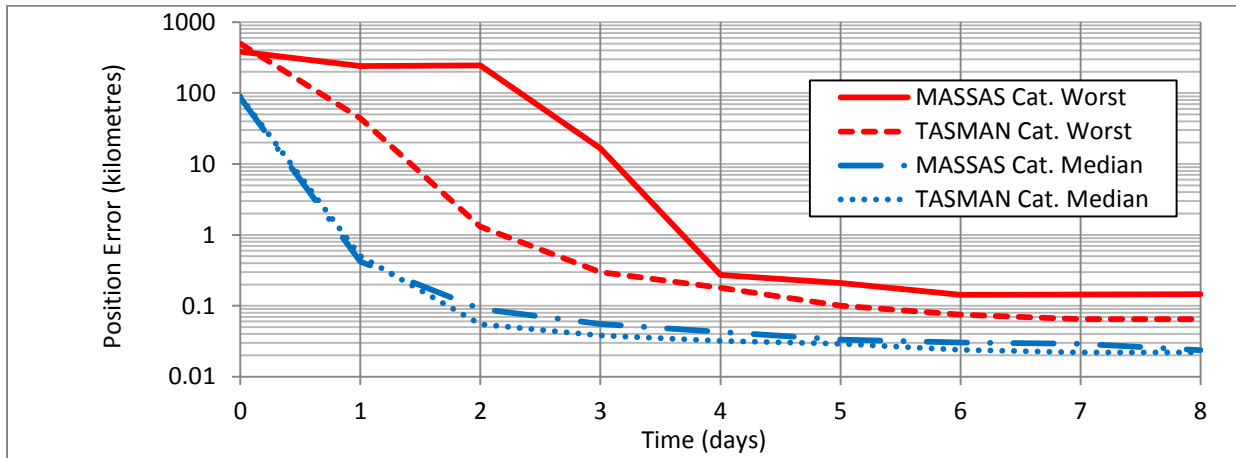
Fig. 3. MASSAS-TASMAN Comparison - Scenario 3

MASSAS's radar model was also tested against its optical model for behavioural comparison. The catalogue was reinitialised to suggested statistical values of σ_P equal to 1×10^{3} m and σ_v equal to 1×10^{-4} ms^{-1}.
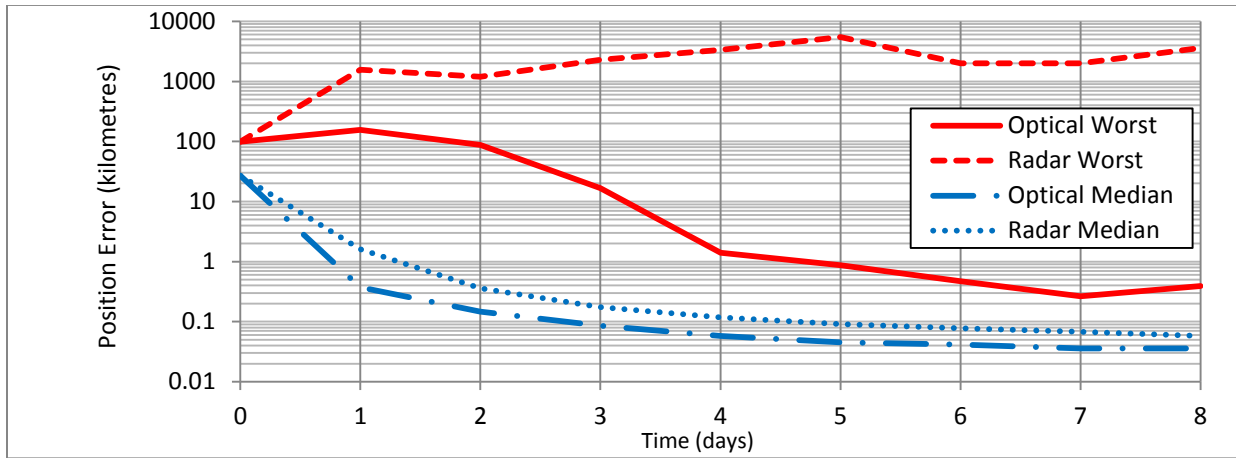
Fig. 4. Optical-Radar Comparison - Scenario 1
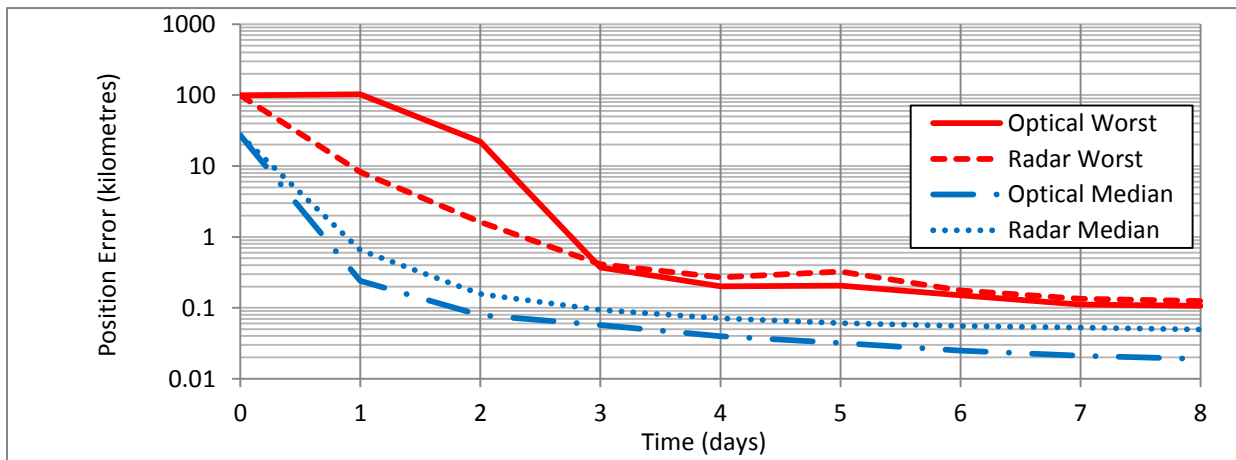
Fig. 5. Optical-Radar Comparison - Scenario 2
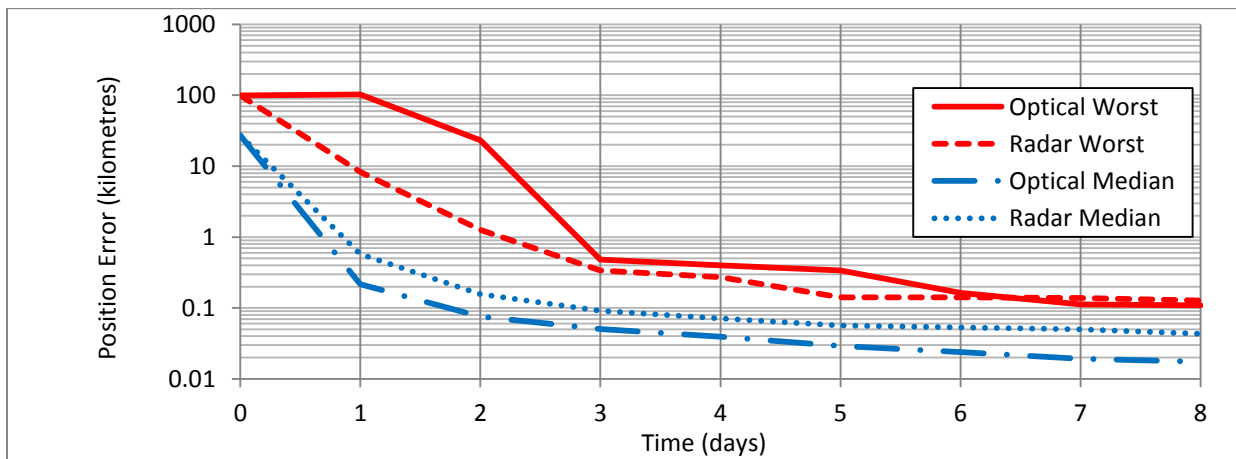
Fig. 6. Optical-Radar Comparison - Scenario 3

Finally error characterization of a mixture of sensors is presented, as well as the inclusion of a fused-sensor. The scenario, location and number of sensors were maintained for the production of these results. Mixed sensor configurations have been labelled Hybrid with a numeric suffix indicating the ratio of optical to radar sensors. The

final sensor labelled Optically Augmented Radar (OAR) is a fused result combining optical and radar measurements for all sensors within the UKF orbit determination computation. Evaluation of β_{red} was similarly augmented to represent the available measurement information. The results presented show the catalogue metrics, Catalogue Worst Case and Catalogue Median for each sensor configuration broken down into three orthogonal error types: In-track error, along the object's velocity vector; cross-track error, parallel to the orbital plain's angular momentum vector $\boldsymbol{h}$; and normal error, the error component orthogonal to the first two components, which is approximately radial for near circular orbits.
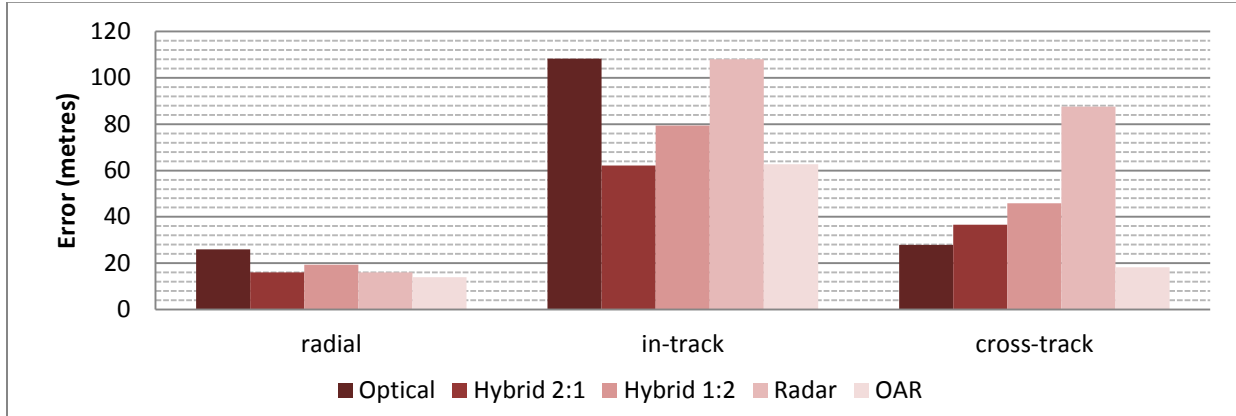
Fig. 7. Sensor Configuration Comparison of Catalogue Worst Case on Day 8 - Scenario 3
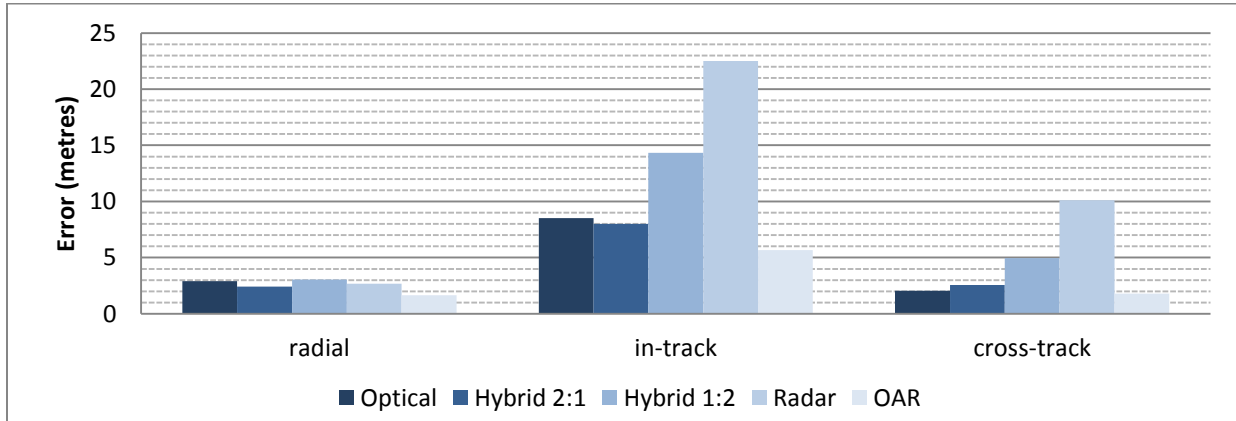
Fig. 8. Sensor Configuration Comparison of Catalogue Median on Day 8 - Scenario 3

5. CONCLUSION

The comparison of results presented in Fig. 1 to Fig. 3 show that both simulation's metrics exhibit greater similarity in Scenarios 2 and 3 than in Scenario 1. Nevertheless, Scenario 1 is the least optimal solution and is most likely to give inconsistent results due to its pseudo-heuristic scheduling regime. The most notable difference between each simulation's Scenario 2 and 3 behaviours is the large difference in the Catalogue Worst Case metric during days 1-2. MASSAS's stunted reduction in Catalogue Worst Case was caused by a complete lack of observability of a small number of objects from any sensor on these two crucial days. Most importantly however, both systems confirm that each scenario is an improvement over its predecessor. At the end of the simulation, MASSAS experienced a 43% improvement in Catalogue Median accuracy between Scenarios 1 and 2 in contrast to TASMAN's 13% improvement. Likewise MASSAS experienced a 12% improvement between Scenarios 2 and 3 which is more similar to TASMAN's 10% improvement.

Fig. 4 through Fig. 6 indicates that under the proposed experimental conditions, optical sensors achieve a Catalogue Median with greater accuracy than radar with an approximate 60% increase for both Scenarios 2 and 3. Scenario 1 produced a reduced yet still significant increase in accuracy of 38%. Conversely, the results also show optical sensing's weakness due to its dependence on passive radiation. Radar's self-reliance on object illumination, enabled it to avoid the stunted reduction in Catalogue Worst Case experienced by optical. This could have significant

repercussions for large catalogues requiring fast covariance reduction. Finally, the results provide further support for the increased effectiveness of each subsequent scenario. This is especially evident in Scenario 1 where the Catalogue Worst Case actually grows due entirely to poor sensor allocation.

Due to Scenario 3's superior performance, it was chosen as the focus for the comparison of multiple sensor configurations presented in Fig. 7 and Fig. 8. The results confirm that radar measurements suffer from a large amount of in-track error and to a lesser extent also suffer from cross-track error. Interestingly, the optical model's range error does not appear significantly larger than radar's when processed through the UKF. The Hybrid 2:1 configuration has proven to be an excellent compromise between the optical-only and radar-only SNSS. Including a single radar sensor significantly reduces the optical visibility limitations exposed by the optical-radar comparisons but does not suffer from such high levels of in-track and cross-track error. The best performance however, was achieved by the OAR sensor. The fused information has exceeded or met the levels of accuracy achieved by all other sensor configurations.

In general, MASSAS's low fidelity result has successfully provided commensurate scenario behaviour to that originally produced on TASMAN. The greatest indication of an influence on the result due any kind of model miss-match is the apparent lack of visibility of a small number of objects by the optical model; which is unobserved in the TASMAN results. Other differences are likely attributed to best-guess initialisation parameters and the variability of each realisation of a stochastic process. The introduction of MASSAS's disparate sensor analysis supports the necessity for further analysis of the benefits of the cooperative use of disparate sensors within an SNSS for the purposes of SSA.

Hill et al. have offered a number of suggestions for the improvement of TASMAN [1], that are equally valid for MASSAS. Some of these include alternative scheduling processes and associated metrics, including different orbital regimes, investigating effects of sensor outages and missed detections, inclusion of search and catalogue maintenance modes as well as satellite characterisation capabilities. Alternative prospective work better aimed at MASSAS and its capabilities should include characterising the benefits of sensor-fusion with alternative measurements and data association strategies. Additionally, MASSAS's speed should be taken advantage of, to explore steady state system behaviour and catalogue building techniques.

6.   REFERENCES

1.   Hill, K. et al, *Covariance-Based Network Tasking of Optical Sensors,* in Proc. AAS/AIAA Space Flight Machanics Meeting, Feb, 2010

2.   USSTRATCOM, *Space Track,* [cited 2011 Mar 3rd]; Available from: www.space-track.org, 2004

3.   Blackman, S.S. and Popoli, R., *Design and analysis of modern tracking systems*. Artech House radar library., Artech House, Boston, 1999

4.   Tapley, B.D. et al, *Statistical orbit determination*, Elsevier Academic Press, Amsterdam; Boston, 2004

5.   Julier, S.J. and Uhlmann, J.K., *A new extension of the Kalman filter to nonlinear systems,* in Proc. AeroSense: 11th Int. Symp. Aerospace/Defence Sensing, Simulation and Controls, 1997

6.   Crassidis, J.L. and Markley, F.L., *Uncented Filtering for Spacecraft Attitude Estimation,* AIAA 2003-5484, AIAA Guidance, Navigation and Control Conference, Austin, Texas, August 11-14, 2003

7.   Simon, D., *Optimal state estimation : Kalman, H∞ and nonlinear approaches*, Wiley-Interscience, Hoboken, N.J., 2006

8.   Vallado, D.A. and McClain, W.D., *Fundamentals of astrodynamics and applications*. 3rd ed. Space technology library, Springer, New York, 2007

9.   Alfriend, K.T. et al, *Orbit Update Comparison Using Optical and Radar Systems,* 2004 AMOS Technical Conference, Maui, HI, September 13-17, 2004